The Plant Cell, Vol. 25: 4391–4404, November 2013, www.plantcell.org

HIGH EXPRESSION OF OSMOTICALLY RESPONSIVE GENES1 Is Required for Circadian Periodicity through the Promotion of Nucleo-Cytoplasmic mRNA Export in *Arabidopsis*[W][OPEN]

Dana R. MacGregor,[a,1] Peter Gould,[b,1] Julia Foreman,[c] Jayne Griffiths,[c] Susannah Bird,[d] Rhiannon Page,[a] Kelly Stewart,[c] Gavin Steel,[c] Jack Young,[b] Konrad Paszkiewicz,[a] Andrew J. Millar,[c] Karen J. Halliday,[c] Anthony J. Hall,[b] and Steven Penfield[a,2]

[a] Biosciences, College of Life and Environmental Sciences, University of Exeter, Exeter EX4 4QD, United Kingdom
[b] Institute of Integrative Biology, University of Liverpool, Liverpool, L69 7ZB, United Kingdom
[c] Centre for Synthetic and Systems Biology (SynthSys), School of Biological Sciences, University of Edinburgh, Edinburgh EH9 3JD, United Kingdom
[d] Department of Biology, University of York, York YO10 5DD, United Kingdom

ORCID IDs: 0000-0003-0543-0408 (D.R.M.); 0000-0003-1756-3654 (A.J.M.).

Cold acclimation has been shown to be attenuated by the degradation of the INDUCER OF CBF EXPRESSION1 protein by the E3 ubiquitin ligase HIGH EXPRESSION OF OSMOTICALLY RESPONSIVE GENES1 (HOS1). However, recent work has suggested that HOS1 may have a wider range of roles in plants than previously appreciated. Here, we show that *hos1* mutants are affected in circadian clock function, exhibiting a long-period phenotype in a wide range of temperature and light environments. We demonstrate that *hos1* mutants accumulate polyadenylated mRNA in the nucleus and that the circadian defect in *hos1* is shared by multiple mutants with aberrant mRNA export, but not in a mutant attenuated in nucleo-cytoplasmic transport of microRNAs. As revealed by RNA sequencing, *hos1* exhibits gross changes to the transcriptome with genes in multiple functional categories being affected. In addition, we show that *hos1* and other previously described mutants with altered mRNA export affect cold signaling in a similar manner. Our data support a model in which altered mRNA export is important for the manifestation of *hos1* circadian clock defects and suggest that HOS1 may indirectly affect cold signaling through disruption of the circadian clock.

INTRODUCTION

Plants sense cold temperatures and mount responses to survive freezing, a process known as cold acclimation. The best characterized molecular genetic pathway regulating cold responses is the *CBF* (for C-repeat binding factor) pathway (Fowler and Thomashow, 2002; Zhu et al., 2004; Chinnusamy et al., 2010). In *Arabidopsis thaliana*, the expression of three of the *CBF* transcription factors *CBF1*, *CBF2*, and *CBF3*, is induced in response to low temperatures (Medina et al., 1999), and constitutive overexpression of these genes is sufficient to increase freezing tolerance (Jaglo-Ottosen et al., 1998; Liu et al., 1998; Sharabi-Schwager et al., 2010). The CBF proteins bind to characterized *cis*-elements in cold-responsive genes to alter their expression and induce pathways enabling cold survival (Stockinger et al., 1997; Gilmour et al., 1998). Cold signaling can also affect *CBF* transcription through calcium signaling (Yang et al., 2010) and calmodulin-binding transcription factor activity (Doherty et al., 2009).

HIGH EXPRESSION OF OSMOTICALLY RESPONSIVE GENES1 (*HOS1*) has been proposed to be a key negative regulator of cold signaling (Ishitani et al., 1998; Lee et al., 2001; Dong et al., 2006a). HOS1 is a large protein that shares sequence similarity with Ring E3 ligases (Lee et al., 2001). In the nucleus, HOS1 attenuates the cold response by the degradation of INDUCER OF CBF EXPRESSION1 (ICE1), a Myc-like basic helix-loop-helix transcription factor that binds the promoter of *CBF3* and is necessary and sufficient for the upregulation of *CBF3* expression in response to cold treatment (Lee et al., 2001; Chinnusamy et al., 2003; Dong et al., 2006a; Miura et al., 2007; Lee et al., 2012). *hos1* mutants show constitutive expression of cold-responsive genes, whereas *HOS1* overexpression leads to a reduction in *CBF* expression and increased sensitivity to freezing (Ishitani et al., 1998; Lee et al., 2001; Dong et al., 2006a). In addition to a role in cold acclimation, HOS1 has more recently been shown to influence the abundance of the photoperiod sensor protein CONSTANS (CO; Jung et al., 2012; Lazaro et al., 2012) and to physically interact with components of the nuclear pore (Tamura et al., 2010).

The plant circadian clock is composed of an interlocking series of transcriptional negative feedback loops, and alterations to the expression of any one of the genes can have profound effects on the levels and timing of the others (Pokhilko et al., 2012). Loss-of-function mutations in *CIRCADIAN CLOCK ASSOCIATED1* (*CCA1*), *LATE ELONGATED HYPOCOTYL* (*LHY*),

[1] These authors contributed equally to this work.
[2] Address correspondence to s.d.penfield@exeter.ac.uk.
The author responsible for distribution of materials integral to the findings presented in this article in accordance with the policy described in the Instructions for Authors (www.plantcell.org) is: Steven Penfield (s.d.penfield@exeter.ac.uk).
[W] Online version contains Web-only data.
[OPEN] Articles can be viewed online without a subscription.
www.plantcell.org/cgi/doi/10.1105/tpc.113.114959

the pseudo-response regulators *PRR5* and *PRR3*, or *TIMING OF CAB EXPRESSION1* (*TOC1*) shorten the period of the circadian clock, whereas loss of *PRR9*, *PRR7*, or *ZEITLUPE* (*ZTL*) lengthen period, and mutations in *GIGANTEA* (*GI*) and the evening complex components *LUX ARRHYTHMO* (*LUX*), *EARLY FLOWERING3* (*ELF3*), or *ELF4* result in a reduction in amplitude and rhythm robustness (Nagel and Kay, 2012). Loss of clock function not only alters the expression of the clock genes themselves, but also has physiological consequences, including altered flowering time (Imaizumi, 2010), growth regulation (Nozue et al., 2007), and plant fitness and vigor (Dodd et al., 2005). The circadian clock is also essential for mounting a cold response (Dong et al., 2011; Seo et al., 2012).

CBF genes themselves are rhythmically expressed (Harmer et al., 2000), and their cold induction is gated by the circadian clock (Fowler et al., 2005). Perturbation of the circadian clock results in altered cold responses in *Arabidopsis* and poplar (*Populus* spp; Nakamichi et al., 2009; Ibáñez et al., 2010; Dong et al., 2011), and cold temperatures profoundly affect clock function (Bieniawska et al., 2008). More interestingly, *CCA1* and *LHY* can transduce cold signals to *CBFs* through a mechanism that promotes cold-regulated alternative splicing (Dong et al., 2011; James et al., 2012; Seo et al., 2012).

HOS1 interacts with *Arabidopsis* structural nuclear pore components and localizes to the nuclear envelope (Tamura et al., 2010; Lazaro et al., 2012), suggesting that HOS1 has a more general function in plant cells. Here, we show that *HOS1* is necessary for normal circadian rhythms and for mRNA export out of the nucleus. We demonstrate that mRNA export is essential for correct periodicity of the circadian clock and that the effects of *hos1* on cold-regulated gene expression and circadian periodicity are shared by nuclear pore mutants previously demonstrated to be required for normal mRNA export. Our results show that *HOS1* affects cold signaling at least in part through altered mRNA export and that this may be mediated by changes in clock gene expression.

RESULTS

HOS1 Is Necessary to Maintain Wild-Type Circadian Clock Periodicity

We screened *hos1-3* and two novel alleles in Columbia (Col; designated *hos1-5* and *hos1-6*; see Methods) for circadian-period defects using delayed fluorescence (Figure 1). Mutants harboring these alleles showed a decrease in the amount of *HOS1* RNA (Figure 1B) and shared the previously described phenotypes of other *hos1* mutants, including early flowering and increases in cold-responsive gene expression such as that of *CBF3* (see Supplemental Figure 1 online; Lee et al., 2001; Lazaro et al., 2012). All three insertion lines exhibited significant lengthening of the clock period compared with the wild type (Figures 1C to 1F). The long-period *hos1* mutant phenotype was observed when plants were grown at 12, 17, or 27°C in either constant red or blue light or in the dark (Figures 1C to 1F; see Supplemental Figure 2 online). Alleles of *hos1* in C24 (*hos1-1*) and Landsberg *erecta* (*hos1-2*) also shared the long-period phenotype (see Supplemental Figure 3 online); therefore, the long-period phenotype of *hos1* is common between all types of alleles and accessions investigated. To demonstrate that this phenotype was not specific to the delayed fluorescence assay, we transformed the *hos1-3* mutant with luciferase (*LUC*) reporter lines under the control of the *CHLOROPHYLL A/B BINDING PROTEIN2* (*CAB2*), *COLD-REGULATED15a* (*COR15a*), or *COLD, CIRCADIAN RHYTHM, AND RNA BINDING2* (*CCR2*) promoter. Compared with the wild type, *hos1-3* had a significantly longer period for all three reporter lines at all temperatures tested (see Supplemental Figure 4 online). *hos1-3* mutants also showed a long-period phenotype for *LHY*:*LUC*, *PRR9*:*LUC*, *PRR7*:*LUC*, and *TOC1*:*LUC* (see Supplemental Figure 5 online). Therefore, *HOS1* is required for the maintenance of circadian period in *Arabidopsis*, and this phenotype is independent of accession, temperature, light quality, or output measured.

hos1 Does Not Require Individual Clock Components for the Observed Long-Period Phenotype

Previously, HOS1 has been shown to exhibit E3 ubiquitin ligase activity and to destabilize the ICE1 or CO proteins through proteasomal degradation targeted by ubiquitination (Dong et al., 2006a; Lazaro et al., 2012). In both of these cases, *hos1* phenotypes are ascribed to the consequences of overaccumulation of the target protein. We took a genetic approach to determine whether *HOS1* requires specific clock components for the long-period phenotype and screened double mutants between *hos1* and eight core clock components for altered rhythms in delayed fluorescence at 12, 17, and 27°C in constant red light (Figure 2). We did not find any clock mutant with a period phenotype that was epistatic to *hos1-3*. Under these conditions, in cases where single clock mutants had little effect on period, double mutants had a period resembling the *hos1-3* single mutant (*cca1 hiking expedition2* [*che-2*], *prr3-1*, and *prr5-11*). Additive interactions were observed between *hos1-3* and *toc1-101*, *lhy-20*, *prr7-11*, and *prr7 prr5* double mutants, whereas *elf3-1* and *gi-201* led to arrhythmic plants in this assay with or without the additional *hos1-3* mutation. Therefore, the *hos1* long-period phenotype is not dependent on misregulation of these individual clock components.

We also tested whether *hos1* mutants had altered hypocotyl elongation, a characteristic shared by multiple circadian clock mutants. In 12-h-light/12-h-dark (12L:12D) white-light cycles or various fluences of constant red or blue light, *hos1* had consistently longer hypocotyls than the wild type, but when grown in the dark, the *hos1* hypocotyls were shorter (see Supplemental Figures 6A to 6E online). Therefore, *HOS1* is required for normal hypocotyl elongation in *Arabidopsis*. We then screened the double mutants for epistasis; all of the double mutant hypocotyls were longer than those of the corresponding single clock mutant in 12L:12D white-light cycles (see Supplemental Figure 6F online) or shorter when grown in the dark (see Supplemental Figure 6G online), suggesting that the *hos1* hypocotyl phenotype cannot be ascribed to overaccumulation of one of these clock proteins. We were unable to isolate double mutants with *cca1* (At2g46830), *prr9* (At2g46790), or *elf4* (At2g40080) mutants because of their genomic proximity to the *HOS1* locus.

To demonstrate that the circadian and hypocotyl phenotypes are caused by the loss of *HOS1*, we created transgenic *hos1-3* lines expressing translational fusions between HOS1 and cyan

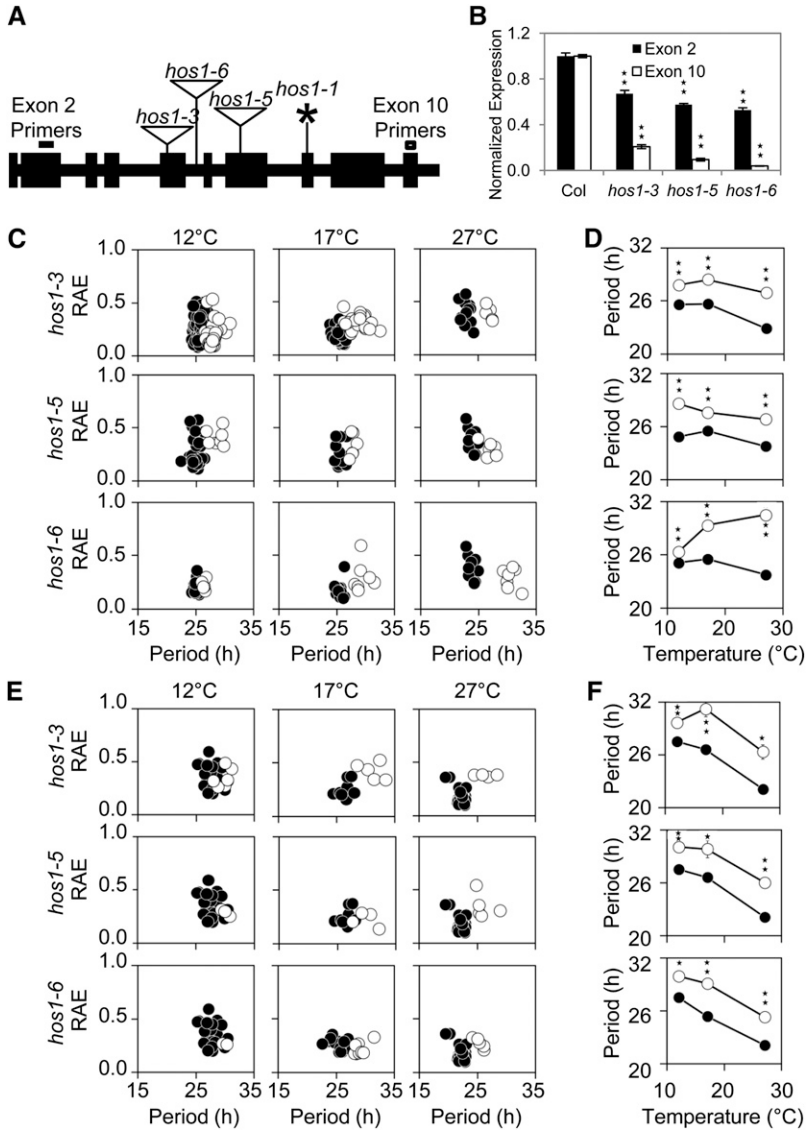

Figure 1. Mutations to *HOS1* Result in a Long-Period Circadian Phenotype across a Range of Physiological Temperatures and Light Conditions.

(A) Schematic diagram showing positions of the *hos1* mutations across the *HOS1* locus. Exons are shown in black boxes and introns in black lines. The position of the *hos1* mutations and allele designations are labeled. Triangles represent T-DNA insertions and the asterisk represents point mutations. The primer positions in exons 2 and 10 are marked to illustrate the positions of qPCR primers used to produce the data in Figure 1B.

(B) qPCR data showing reduced levels of *HOS1* mRNA expression in each of the *hos1* mutants studied. Primers for exon 2 (dark gray bars) are located upstream of and exon 10 (white bars) are located downstream of all *hos1* mutations studied (see **[A]**). Seedlings were grown for 10 d before being harvested at dawn. Data are averages of biological triplicate ± SE normalized for transcript abundance to UBQ10. Stars indicate significant difference to the respective wild type as measured by Student's *t* test where one star indicates $P \leq 0.05$ and two stars $P \leq 0.01$.

(C) to **(F)** Delayed fluorescence assays comparing the wild type (Col) to the *hos1* alleles. Seedlings were entrained for 7 d in 12L:12D white-light cycles at 22°C before transfer to experimental conditions of constant 12, 17, or 27°C and constant red light (**[C]** and **[D]**) or constant blue light (**[E]** and **[F]**). Delayed fluorescence was then measured in several *hos1* mutants (white circles) compared with wild-type data (Col, black circles).

(C) and **(E)** Plots showing period estimations produced via mathematical analysis plotted versus RAE for the wild type (Col) versus the *hos1* mutants. Data are from individual wells containing 10 to 20 seedlings.

(D) and **(F)** Plot illustrating the effect of temperature on the variable weighted mean of the period for the wild type (Col) versus *hos1* mutants. Data are variable weighted mean ± SE. Stars indicate significant difference to the respective wild type as measured by Student's *t* test where one star indicates $P \leq 0.05$ and two stars $P \leq 0.01$.

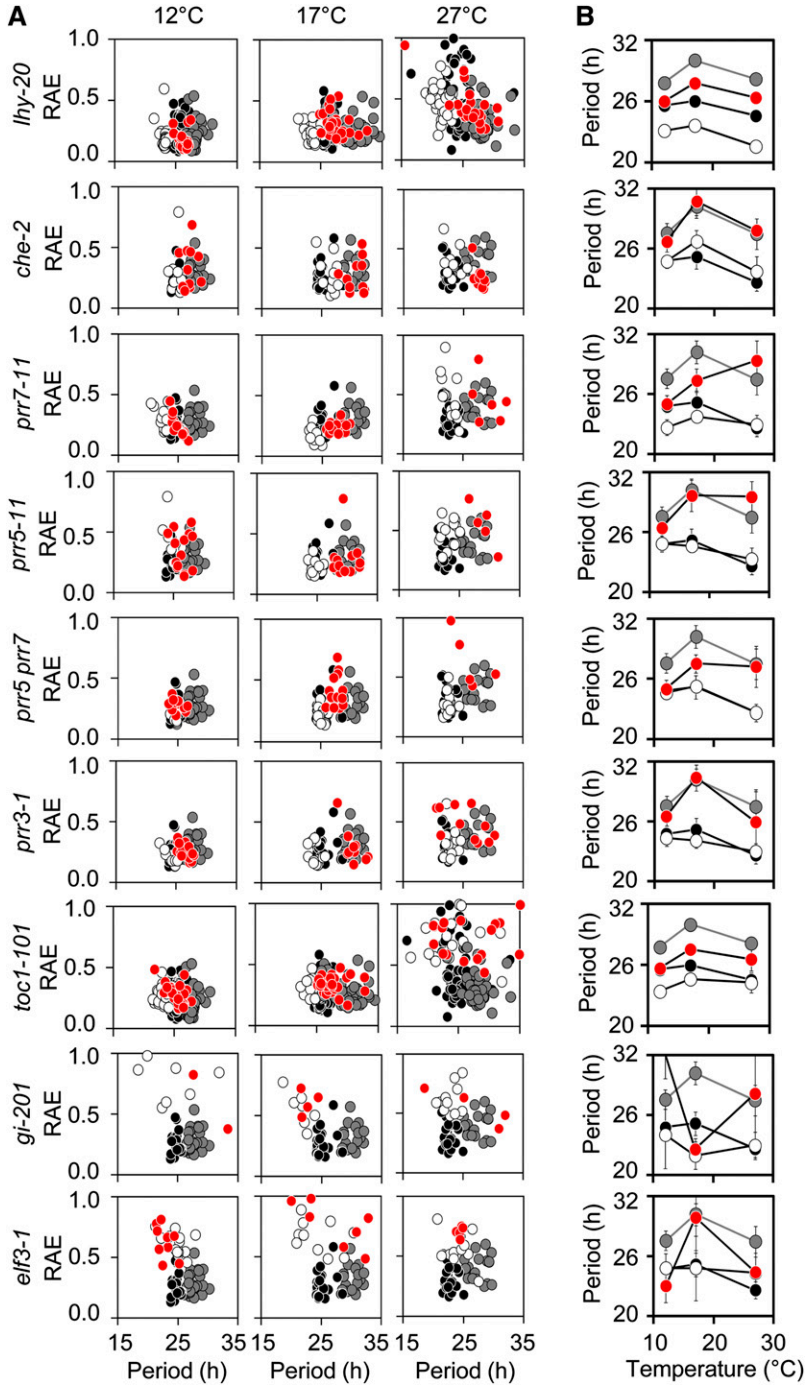

Figure 2. The Long-Period Phenotype in *hos1* Does Not Require Selected Individual Clock Components.

(A) Delayed fluorescence assays comparing the wild type (Col, black circles) to *hos1* (gray circles) and the single (white circles) and double (red circles) mutants. Seedlings were entrained for 16 d in 12L:12D white-light cycles at 22°C before transfer to experimental conditions of constant 12, 17, or 27°C and constant red light. Plots show period estimations produced via mathematical analysis plotted versus RAE. Data are from individual wells containing 10 to 20 seedlings.

(B) Plots illustrating the effect of temperature on the variable weighted mean of the period for the wild type (Col, black circles) to *hos1* (gray circles) and the single (white circles) and double (red circles) mutants. Data are variable weighted mean ± SE. Stars indicate significant difference to the respective wild type as measured by Student's *t* test where one star indicates $P \leq 0.05$ and two stars $P \leq 0.01$.

fluorescent protein (CFP) under the 35S promoter and demonstrated the HOS1-CFP fusion protein fully complemented both the *hos1-3* hypocotyl and period phenotypes (see Supplemental Figure 7 online).

hos1 Mutants Show Protein and Promoter Rhythms Despite Poor mRNA Rhythm Robustness

To determine if *HOS1* is required for proper expression of the core components of the circadian clock, RNA from the wild type and *hos1-3* was sampled every 2 h from seedlings growing in constant red light or 12L:12D red-light cycles (see Methods). Based on the analysis of previous long-period circadian clock mutants, we expected the period of clock gene expression to be lengthened and/or alterations in the amplitudes of expression for some genes. However, the effects of *hos1-3* on clock gene expression were inconsistent with a typical long-period mutant (Figure 3; see Supplemental Figure 8 online). In *hos1-3*, the amplitude and rhythmicity of expression of the circadian clock genes was significantly affected after 2 d in constant conditions (Figure 3). Notable features under constant conditions were the reduction in amplitude of *CCA1*, *LHY*, and *PRR7*, whereas *PRR9*, *TOC1*, *GI*, *LUX*, and *ELF3* expression showed little evidence of rhythmicity (Figure 3). In 12L:12D red-light cycles, the most prominent effect of *hos1-3* was on the amplitude of expression, where, for instance, at 17°C the maximal expression of *LHY*, *CCA1*, and *PRR5* was reduced and peak expression of *PRR9*, *PRR7, TOC1*, and *ELF3* was increased (see Supplemental Figure 6 online). The phase of peak expression in diurnal conditions was largely unaffected in *hos1-3* (see Supplemental Figure 8 online). Overall patterns of expression were similar when the plants were grown at 27, 22, 17, or 12°C (see Supplemental Figure 8 online). These analyses indicate that *HOS1* is required not only for regulation of cold signaling (Ishitani et al., 1998; Lee et al., 2001; Dong et al., 2006a) and flowering time genes (Lazaro et al., 2012) but also for correct expression of the core circadian clock genes at all these temperatures and for robust mRNA rhythms in constant conditions.

Transcript analysis showed that *hos1* exhibited poor mRNA rhythms, whereas delayed fluorescence and promoter:LUC data were rhythmic, albeit with a long period and lowered amplitude. To determine if protein rhythms continue in the *hos1* mutant, we measured LHY protein abundance as well as LHY target gene expression and promoter activity under conditions matching those for the clock gene mRNA study in Figure 3. Quantitative PCR (qPCR) revealed that endogenous *CAB2* and *CCR2* mRNA rhythms were markedly less robust with no detectable oscillations after 80 h under constant red light, in common with *LHY* (Figure 4A). By contrast, *LHY:LUC*, *CAB2:LUC*, and *CCR2:LUC* all oscillated with a long period in *hos1-3* (Figures 4B and 4C). LHY protein levels oscillated with a long period (Figure 4D), and

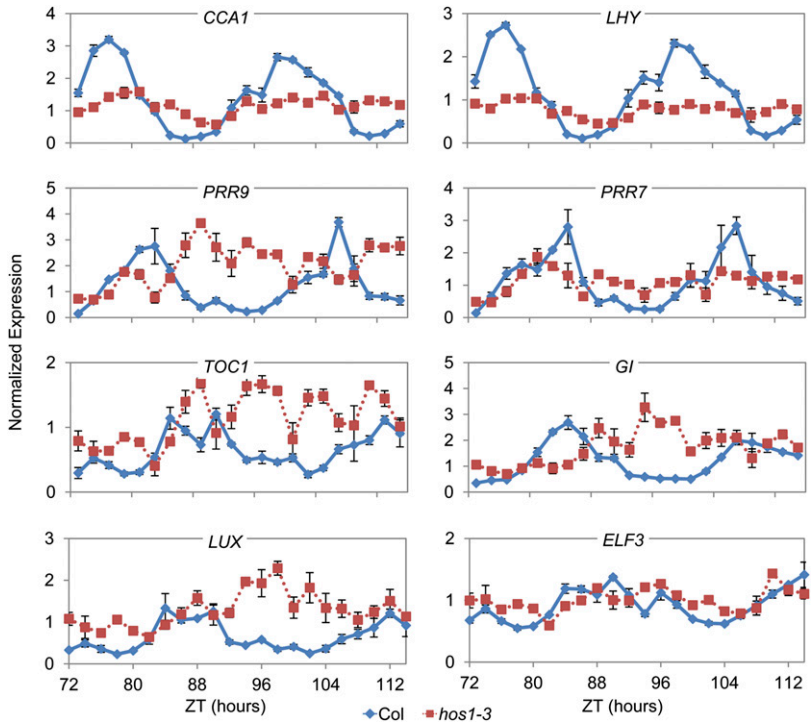

Figure 3. Under Constant Red Light, *HOS1* Is Required for Correct Expression of Clock Genes.

Plants were grown for 7 d under 12L:12D white-light cycles at 22°C followed by 2 d in 12L:12D red-light cycles at 17°C before being transferred to constant red light at 17°C for sampling in biological triplicate at the Zeitgeber time (ZT) times indicated. The cDNA were analyzed by qPCR three times for each biological replicate. Data presented are the average of three biological repeats ± SE. Transcript abundance levels were normalized to *ACT7*. Blue diamonds with solid lines are data from the wild type (Col), whereas red squares with dotted lines are data from *hos1-3*.

we observed reduced LHY protein levels in *hos1-3* as would have been predicted by the observed reduction in *LHY* mRNA abundance (Figure 4A). Taken together, our evidence suggests that mRNA rhythms are most strongly affected by the *hos1* mutation and that clock protein abundance and promoter activity exhibit more robust rhythms, although with a long period.

hos1 Accumulates Polyadenylated mRNA in the Nucleus

From our expression analysis of core clock genes, it is clear that *hos1* alters clock gene mRNA amplitude. Therefore, we speculated that HOS1 may be playing a functional role in regulating the abundance of clock mRNA. In a proteomic screen, HOS1 interacts with the nuclear pore proteins RNA EXPORT FACTOR1–green fluorescent protein (GFP) and the nucleoporin Nup43-GFP (Tamura et al., 2010) and associates with the nuclear periphery (Lazaro et al., 2012). Nuclear pore complexes are required for the export of mRNA from the nucleus; mutating components of the nuclear pore complex results in abnormal mRNA export as shown by in situ hybridization against poly(A)-containing mRNA (Dong et al., 2006b; Parry et al., 2006; Wiermer et al., 2012). Therefore, we used in situ hybridization to detect poly(A)-containing mRNA to determine if *HOS1* plays a role in nucleo-cytoplasmic mRNA export. Like the previously described *los4-1* mutant (Gong et al., 2002, 2005), *hos1* plants exhibited increased nuclear retention of poly(A)-containing RNA in the nuclei compared with the appropriate wild-type control (Figure 5). There was no difference in the in situ fluorescence when fixation was performed at dawn compared with dusk in either wild-type or *hos1-3* samples, and no significant accumulation of signal was observed in another long-

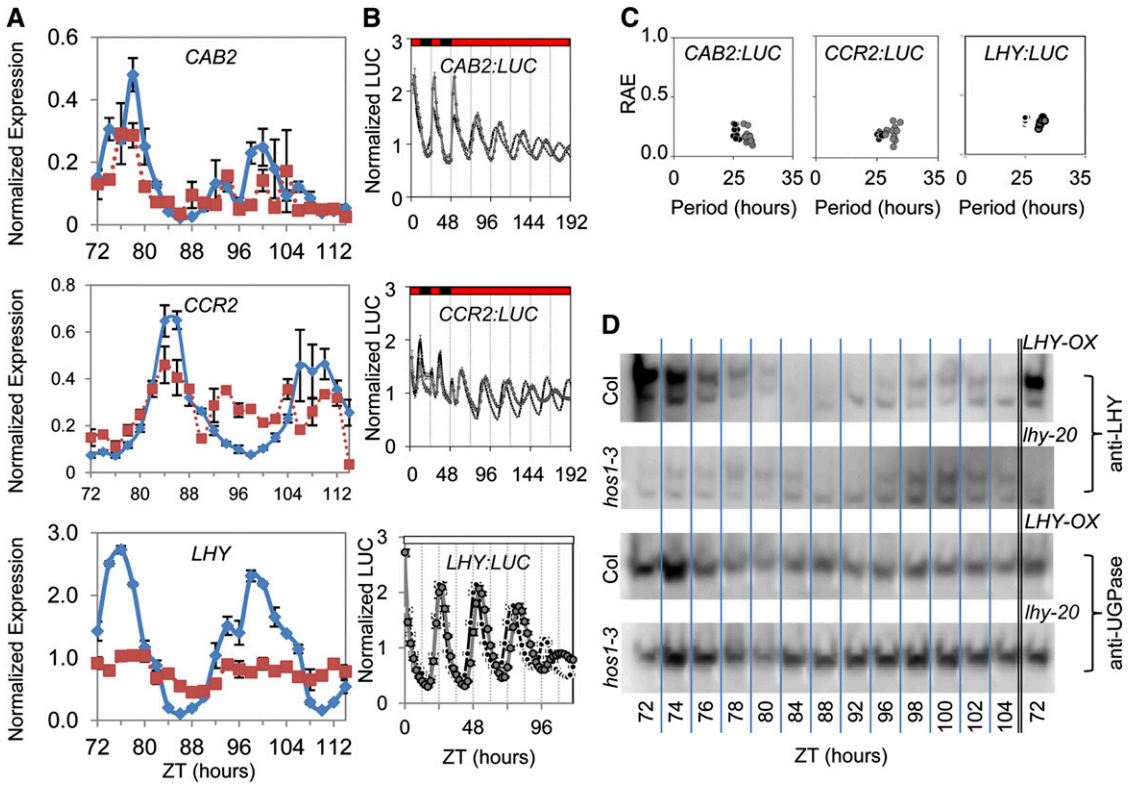

Figure 4. *hos1* Mutants Exhibit Long Period but Robust Protein and Promoter Rhythms Despite Poor mRNA Rhythm Robustness.

(A) The expression of endogenous *CAB2*, *CCR2*, and *LHY* in the wild type (Col) and *hos1-3* in constant red light (see Methods). Data are the average of the three biological repeats ± SE. Transcript abundance levels were normalized to *ACT7*. Samples were taken at the Zeitgeber time (ZT) indicated. Blue diamonds are data from Col, whereas red squares show data from *hos1-3*.

(B) Plots to show the normalized mean *CAB2:LUC*, *CCR2:LUC*, and *LHY:LUC* luminescence profiles for the wild type and *hos1-3* mutant. Data are presented as means ± SE. Transgenic seedlings containing the *CAB2:LUC* or *CCR2:LUC* reporter were entrained for 7 d in 12L:12D white-light cycles at 22°C before transferred to experimental conditions of constant 17°C and 2 d of 12L:12D red-light cycles followed by 6 d of constant red light. Transgenic seedlings containing the *LHY:LUC* reporter were entrained for 6 d in 12L:12D white-light cycles at 22°C before transferred to experimental conditions of constant white light at room temperature. *hos1-3* (gray filled circles) is compared with wild-type data (black filled circles).

(C) Plots to show the period estimations for *CAB2:LUC*, *CCR2:LUC*, and *LHY:LUC* versus RAE for the wild type versus the *hos1-3* mutant.

(D) Immunoblot analysis showing endogenous LHY levels in the wild type (Col) compared with *hos1-3*, with *LHY-OX* and *lhy-20* lines as positive and negative controls, respectively. The blots were reprobed using an antibody against UGPase for the loading control. Plants were grown for 7 d under 12L:12D white-light cycles at 22°C followed by 2 d in 12L:12D red-light cycles at 17°C before being transferred to constant red light at 17°C for sampling at the Zeitgeber time (ZT) times indicated. These images are representative images from technical duplicates.

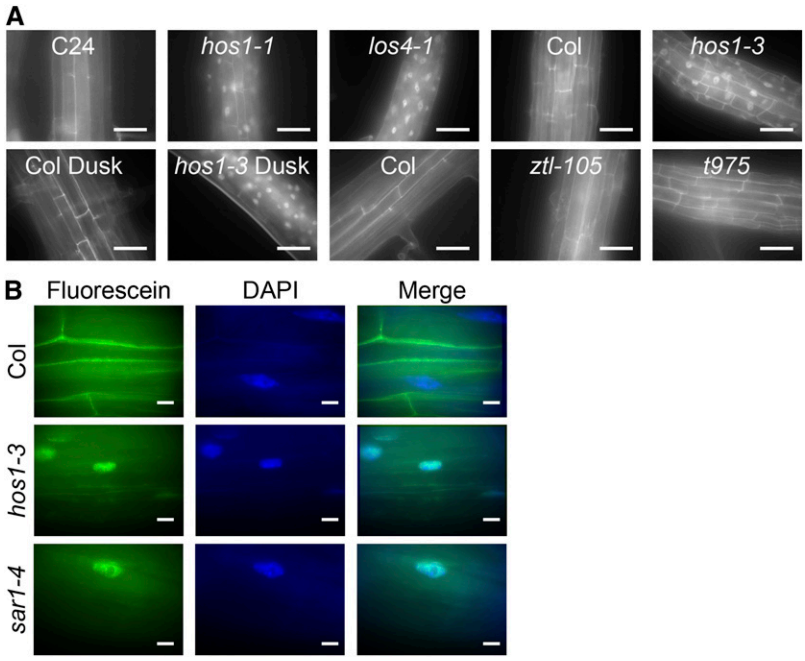

Figure 5. HOS1 Is Required for Nucleo-Cytoplasmic mRNA Export.

(A) In situ hybridization with a fluorescein-labeled oligo(dT) probe in wild-type, *hos1*, *los4*, *ztl* (long period), and *toc1 prr9 prr7 prr5* (*t975*) quadruple mutant (arrhythmic) roots. Plants were fixed at dawn (unless otherwise indicated) after 2 weeks of growth under 12L:12D white-light cycles. Bars = 50 μm.
(B) In situ hybridization with a fluorescein-labeled oligo(dT) in wild-type, *hos1*, and *sar1* roots counterstained with DAPI. Bars = 10 μm.

period mutant, *ztl-105*, or the arrhythmic *toc1 prr5 prr7 prr9* quadruple mutant (Figure 5). Our data therefore suggest that while HOS1 is required for normal mRNA export, this occurs independently of the circadian clock.

To determine if the increased signal observed in the in situ hybridization was due to retention of a small number of mRNA species to a high degree or a low-level retention of many genes, RNA sequencing was performed using samples harvested at dawn (see Methods). Of the total 15,070 genes present, 1308 were upregulated in *hos1-3* compared with the wild type, and 126 were downregulated twofold or more (Table 1; see Supplemental Data Set 1 online). AmiGO analysis (Carbon et al., 2009) of these up- or downregulated genes showed that they fell into a wide range of Gene Ontology classifications (see Supplemental Data Set 2 online). This analysis shows that *hos1* mutants exhibit a profound misregulation of a large number of genes, most of which are mildly upregulated. This effect is consistent with the expected consequences of transcripts being retained in the nucleus, as in eukaryotes mRNA degradation takes place in the cytoplasm (Tourrière et al., 2002). Of the 12 genes that make up the core circadian clock machinery (Pokhilko et al., 2012), seven genes were significantly upregulated and none were significantly downregulated in the RNA sequencing data set at dawn (Table 1; the numerical values for *LHY*, *CCA1*, and *PRR9* were lower in *hos1-3* compared with the wild type but failed significance testing). Using qPCR, we were able to verify that expression of *PRR5*, *TOC1*, *LUX*, *ELF4*, and *ELF3* were upregulated in *hos1*-3 at dawn (Figure 6). The upregulation of these genes in *hos1-3* was also observed in the diurnal data set in Supplemental Figure 8 online even though these genes were lowly expressed at dawn when this sampling occurred, as would be expected for evening-phased genes. These upregulated clock genes were predominantly evening-expressed

Table 1. Loss of HOS1 Results in Large Numbers of Upregulated Genes

Category	Upregulated in *hos1-3*	Downregulated in *hos1-3*
Total number of genes	1308	126
Expressed C+E union	832	49
Circadian C+E union	400	35
Genes circadian expressed (%)	48.1	71.4
Differentially expressed clock genes	*PRR5*, *PRR3*, *TOC1*, *LUX*, *ELF3*, *ELF4*, *CHE*	None

Genes that are downregulated are also dominated by circadian-expressed genes. Analysis of RNA sequencing shows that reads map to 15,070 genes expressed in the *hos1* mutant at dawn. C+E union refers to the list of circadian-expressed genes defined by Covington et al. (2008). Significant gene expression differences were calculated by Cufflinks (Trapnell et al., 2012).

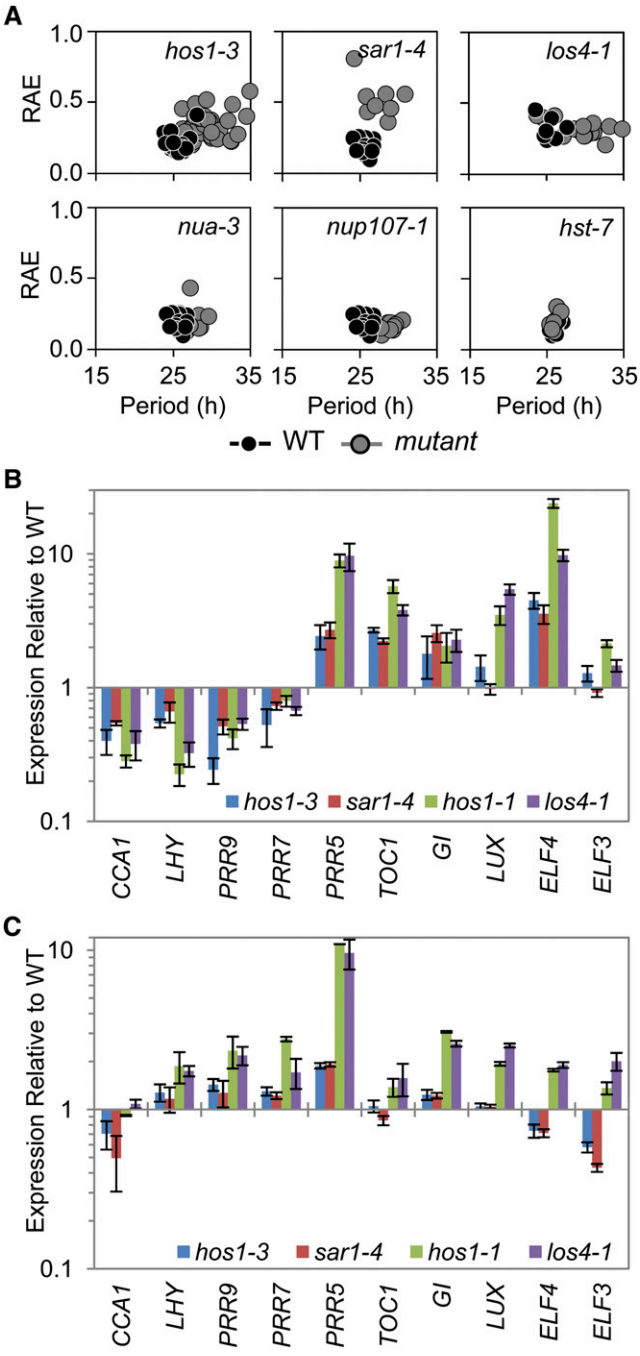

Figure 6. Mutants Resulting in Altered mRNA Export Exhibit Long-Period Circadian Phenotypes and Alterations to Clock Gene Expression Similar to *hos1*.

(A) Delayed fluorescence was performed on a range of nuclear pore–associated mutants. Seedlings were grown in 12L:12D white-light cycles for 16 d prior to transferring to constant 17°C and constant red light for analysis. Each plot shows period estimations plotted versus RAE comparing the wild type (WT; black circles) and mutant (gray circles).

(B) and **(C)** RNA analysis comparing the expression of clock genes in *hos1* alleles, *sar1-4* and *los4-1*, to their appropriate wild types. Plants were grown for 2 weeks in 12L:12D white-light cycles and harvested in triplicate at dawn CT0 **(B)** or dusk CT12 **(C)**. Data are shown relative to the wild-type values for comparison. Data are averages of biological triplicate ± SE normalized for transcript abundance to *TUB9* **(B)** or *UBQ10* **(C)**. Bar colors are as follows: *hos1-3*, blue; sar*1-4*, red; *hos1-1*, green; and *los4-1*, purple.

transcriptional inhibitors, which may explain the fact that 71% of the genes downregulated in *hos1-3* had circadian expression patterns (Table 1). Of the 1308 genes that were upregulated in *hos1*, 48.1% of those were classified as circadian as analyzed by Covington et al. (2008); this figure is not far from the calculated value of 41.4% circadian-expressed genes within the whole genome (Covington et al., 2008). Therefore, we suggest that loss of *HOS1* directly causes upregulation of gene expression of a large percentage of the genome through mRNA retention but that the genes downregulated in *hos1* are more likely to be affected indirectly through the perturbation of circadian function.

Normal Nucleo-Cytoplasmic mRNA Export Is Required for Circadian Periodicity and Expression of Clock Genes

To determine if the altered nuclear mRNA export is responsible for the long-period phenotype observed in *hos1*, we assessed the circadian period of four further lines in which nuclear pore function is compromised: *suppressor of axr1* (*sar1-4*), *low expression of osmotically responsive genes4* (*los4-1*), *nuclear pore anchor* (*nua-3*), and the recently identified nucleoporin mutant *nup107-1. SAR1*, *LOS4*, and *NUA* are all required for correct mRNA nuclear export (Cernac et al., 1997; Gong et al., 2002, 2005; Dong et al., 2006b; Parry et al., 2006; Xu et al., 2007), and *NUP107* is a structural nucleoporin that is part of the evolutionarily conserved Nup107-Nup160 subcomplex with *SAR1* (Tamura et al., 2010; Clever et al., 2012). In a manner resembling *hos1* mutants, loss of any of these genes led to a long period, as measured by delayed fluorescence (Figure 6A). To demonstrate that the effect on period lengthening was specific to mRNA export, we tested the *hasty* mutant (*hst-7*), the *Arabidopsis* ortholog of the importin β-like proteins that are involved in nucleo-cytoplasmic transport of microRNAs (Bollman et al., 2003; Park et al., 2005). We found that the *hst-7* mutant had a wild-type period (Figure 6A). In further support of the role of mRNA export in proper regulation of the circadian clock, the expression of the core circadian clock components was altered in a similar manner in *los4-1* or *sar1-4* at dawn (Figure 6B) or dusk (Figure 6C) compared with the appropriate wild type. Our results therefore show that period lengthening is a general consequence of disrupting nucleo-cytoplasmic mRNA export in plants and reveal that *hos1* mutants have a period defect resulting from an RNA export defect.

Cold Signaling Is Similarly Perturbed by *hos1*, *sar1*, and *los4*

Although loss of *HOS1*, *LOS4*, or *SAR1* have been shown to result in altered cold responses (Ishitani et al., 1998; Gong et al., 2002, 2005; Dong et al., 2006a, 2006b), these studies have not shown that mutations in these genes lead to similar effects on cold-responsive gene expression. One possibility is that timing of analyses may significantly affect the outcome of experiments, as the cold-signaling genes being monitored are under circadian regulation

(Harmer et al., 2000; Kreps et al., 2002), and loss of these nuclear pore components alters circadian function (Figure 6). Therefore, to determine whether cold signaling was perturbed similarly in these mutants, we examined the expression of cold-signaling genes in these mutants in parallel. Expression of *CBF3* and *RESPONSIVE TO DESSICATION29A* (*RD29A*) was assayed at 0, 8, and 12 h after dawn in seedlings grown in 12L:12D white-light cycles at 22°C (Figures 7A to 7D). The mutations in *los4* or *sar1* led to similar increases in the expression of *CBF3* and its target gene *RD29A* as observed in *hos1* when compared with their wild types. Therefore, when assayed in parallel, the *hos1*, *sar1*, and *los4* mutants display comparable perturbations of cold-responsive gene expression.

It has been recently demonstrated that differential splicing events occur within *LHY* in response to cold stress and that plants incubated at 4°C have an increased proportion of a nonfunctional isoform of *LHY* in which exon E5a is retained (James et al., 2012). We tested the hypothesis that altered cold signaling in *hos1* mutants was due to misexpression of *LHY* by comparing *CBF3* and *RD29A* expression in *hos1* and *hos1-3 lhy-20* double mutants that therefore lack both isoforms of *LHY* (Figures 7E and 7F). Expression of these genes in the double mutant was intermediate between that in *lhy* and *hos1*, showing that the mechanisms that regulate alternative splicing of *LHY* alone do not account for the increase in cold-induced gene expression in the *hos1* mutant. This work shows that HOS1 affects cold signaling through a pathway that does not require *LHY*.

DISCUSSION

The circadian clock requires the rhythmic synthesis and degradation of mRNAs encoding transcriptional regulators in plants. Here, we show that loss of *HOS1* results in period lengthening and the inability to maintain normal mRNA rhythms under constant conditions (Figures 1 and 3; see Supplemental Figures 1 to 5 online). The *hos1* long-period phenotype is shared by four different mutants known to disrupt the nuclear pore complex and/or mRNA export (Figure 6), and we demonstrate that *hos1* mutants constitutively accumulate polyadenylated mRNA in the nuclei (Figure 5). These data, together with the double mutant analysis (Figure 2; see Supplemental Figure 6 online), suggest that the *hos1* circadian defect is due to the loss of nucleo-cytoplasmic mRNA transport, rather than to an interaction with a specific clock protein. Demonstrating the specificity of the nuclear defect, *los4*, *sar1*, and *nua*, which share *hos1*'s long-period phenotype (Figure 6A), are unable to export mRNA to the cytoplasm at normal rates (Figure 5; Gong et al., 2005; Parry et al., 2006; Xu et al., 2007), whereas the *hst-7* mutant, which affects microRNA rather than mRNA export (Bollman et al., 2003), showed no circadian clock phenotype (Figure 6A). Therefore, we conclude that a nucleo-cytoplasmic mRNA export defect results in the circadian clock defect observed in *hos1* mutants.

It is interesting to note that constitutive overexpression of *HOS1* does not result in either circadian arrhythmia or a short period, as occurs for many clock components (reviewed in McClung, 2006); instead, *HOS1* overexpression rescues the clock defect in *hos1-3* to an approximately wild-type period (see Supplemental Figure 7 online). This observation is therefore not consistent with *HOS1* playing a central role in the circadian clock. This work also shows that *hos1* affects signaling and gene expression by mechanisms other than or in addition to the degradation of specific proteins such as ICE1 and CO (Dong et al., 2006a; Lazaro et al., 2012). Currently it is not clear whether the E3 ubiquitin ligase activity of HOS1 is necessary for its role in the promotion of mRNA export. Double mutant analysis suggests that *HOS1* modifies the delayed fluorescence and hypocotyl elongation phenotypes observed in the clock genes analyzed (Figure 2; see Supplemental Figure 6 online), suggesting that *HOS1* may not act on the circadian clock through one specific component. However, double mutants with all clock genes could not be isolated due to the close genomic proximity of *HOS1* with *CCA1*, *PRR9*, and *ELF4*. Thus, it remains possible that *hos1* could show a strong genetic interaction with these mutants.

Although the *hos1* long-period phenotype is shared by mutants lacking four different nuclear pore-associated proteins, it is not clear precisely how disruption of mRNA export affects

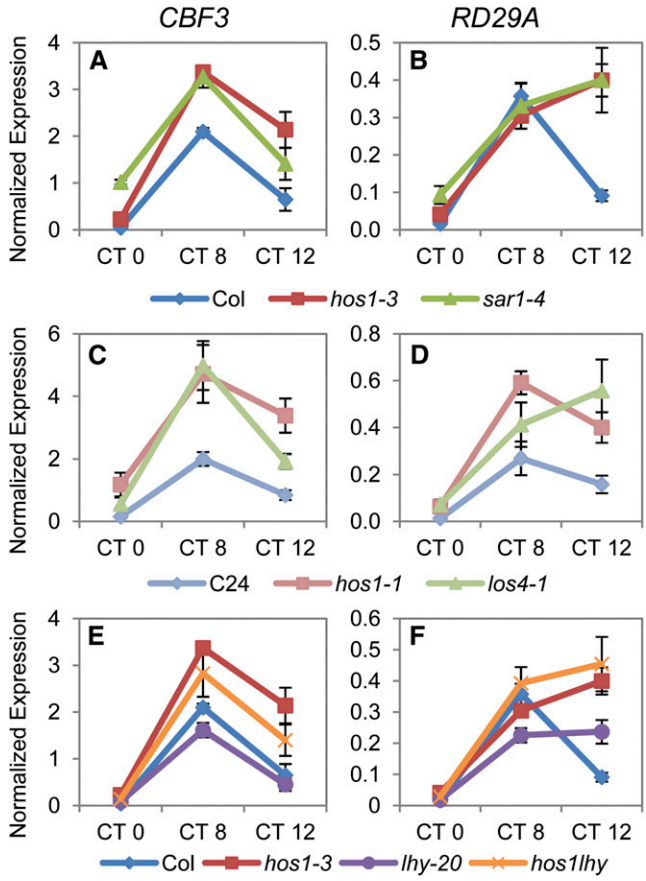

Figure 7. Expression of Cold Signaling Genes Analyzed in Parallel Indicates Similar Perturbations in *hos1* as in *sar1-4* and *los4-1* and This Perturbation Does Not Require LHY.

Expression analysis of *CBF3* (**[A]**, **[C]**, and **[E]**) and *RD29A* (**[B]**, **[D]**, and **[F]**) in the wild type (Col, dark-blue diamonds; C24, light-blue diamonds), *hos1* alleles (*hos1-3*, red squares; *hos1-1*, pink squares), mRNA export mutants (*sar1-4*, dark-green triangles; *los4-1*, light-green triangles), *lhy* (*lhy-20*, purple circles), and *hos1-3 lhy-20* double mutants (*hos1lhy*, orange Xs). Plants were grown for 2 weeks under 12L:12D white-light cycles and harvested at dawn (CT0), 8 h after dawn (CT8), or at dusk (CT12). Data are averages of biological triplicate ± SE normalized for transcript abundance to *UBQ10*.

period. A simple explanation would be that altered export of clock gene RNAs results in a reduced ability to maintain period and rhythms of mRNA abundance. In *hos1* mutants, gross changes in the transcriptome were revealed by RNA sequencing, affecting genes in multiple functional categories rather than specifically circadian- and cold-regulated processes. Because LHY protein rhythm and target-gene promoter activity appear more rhythmic than those of the corresponding mRNAs (Figure 4), our data strongly suggest that *hos1* mutants are disrupted in circadian rhythms primarily because of alterations occurring at the RNA level. The best explanation for the unusual *hos1* circadian phenotype is that because protein synthesis occurs in the cytoplasm, as long as a rhythm of mRNA export is maintained, is it possible to get long-period oscillations of promoter:LUC and protein levels without robust total mRNA rhythms. Furthermore, as we measured total mRNA, which includes RNA retained in the nucleus as well as that in the cytoplasm, it is possible that the population that is available for translation is sufficiently rhythmic in *hos1* to drive oscillations. An effect of *hos1* on circadian protein nuclear import is unlikely in our view, as *Saccharomyces cerevisiae* mutants defective in nuclear protein import are not viable: Indeed, early embryo-lethal pore mutants have been described in *Arabidopsis* (Braud et al., 2012).

Loss of *HOS1*, *LOS4*, or *SAR1* have all been reported to result in altered cold responses; however, the effects of the mutations do not give consistent phenotypes, including two alleles of *LOS4* with apparent opposite alterations to cold-signal transduction (Ishitani et al., 1998; Gong et al., 2002, 2005; Dong et al., 2006a, 2006b). Here, we show that when analyzed together, two *hos1* alleles, *los4* and *sar1*, all show similarly altered cold signaling; expression of *CBF3* and *RD29A* are upregulated in each mutant when assayed 8 to 12 h after dawn (Figures 7A to 7D). Expression of cold-signaling genes, including *CBF3* and *RD29A*, is under circadian control, with maximal expression occurring at 8 to 12 h after dawn (CT8 to CT12) (Harmer et al., 2000; Mockler et al., 2007). Because circadian function is disrupted in mutants with aberrant mRNA export (Figure 6A), and the circadian clock is required for normal cold responses (Dong et al., 2011; Seo et al., 2012), one possibility is that cold signaling is perturbed as a consequence of altered circadian function. Our analysis of *hos1-3 lhy-20* double mutants reveals an intermediate effect on *CBF3* and *RD29A* expression (Figures 7F and 7G), showing that if *HOS1* does affect cold signaling in part through the clock, then this pathway is not solely dependent on *LHY*. Analysis of *hos1 lhy cca1* triple mutants could confirm that cold-signaling defects in *hos1* mutants do not result from the interaction between mRNA export and circadian clock function.

los4 and *sar1* mutants share a suite of phenotypes with *hos1* plants, including early flowering (see Supplemental Figure 1 online; Ishitani et al., 1998; Gong et al., 2005; Parry et al., 2006; Lazaro et al., 2012), defective cold signaling (see Supplemental Figure 1 online; Figure 7; Ishitani et al., 1998; Lee et al., 2001; Gong et al., 2005; Dong et al., 2006a, 2006b), and circadian rhythms (Figure 6). This suggests that these phenotypes share a common cause. Our data show that loss of *HOS1* causes mRNA retention and this has large consequences for gene expression in *hos1* mutants. Further studies of abiotic signaling pathways need to discriminate between the direct and indirect mechanisms through which alterations to these proteins result in the phenotypes and gene expression changes observed.

METHODS

Plant Materials

The genotypes and accessions described herein are as follows. The wild types are Col, C24 expressing *RD29A:LUC* (C24) (Ishitani et al., 1997), or Landsberg *erecta*. The *hos1* mutants are *hos1-1* (Ishitani et al., 1998), *hos1-2* (Lazaro et al., 2012), *hos1-3* (SALK_069312), *hos1-5* (SALK_131629), and *hos1-6* (SALK_052108). Circadian clock mutants used have been described and are *lhy-20* (Michael et al., 2003), *che-2* (Pruneda-Paz et al., 2009), *prr9-10* (Ito et al., 2003), *prr7-11* (Yamamoto et al., 2003), *prr5-11* (Yamamoto et al., 2003), *prr3-1* (Para et al., 2007), *toc1-101* (Kaczorowski, 2004), *gi-201* (Martin-Tryon et al., 2007), *lux-5* (Hazen et al., 2005), *elf3-1* (Hicks et al., 1996), and *ztl-105* (SALK-069091) (Martin-Tryon et al., 2007). Previously published mRNA export mutants were obtained from the Nottingham Arabidopsis Stock Centre and have been previously described: *sar1-4* (SALK_126801) (Parry et al., 2006), *los4-1* (Gong et al., 2005), *nua-3* (SAIL_505_H11) (Xu et al., 2007), *nup107-1* (SALK_057072) (Wiermer et al., 2012, Clarkson et al., 1997), and *hst-7* (Bollman et al., 2003).

Growth Conditions

For RNA extraction, hypocotyl measurements, confocal microscopy, and mRNA retention, experiments seeds were surface sterilized and stratified at 4°C for 2 to 4 d on Murashige and Skoog (MS) agar (Melford) and 0.9% agar (Sigma-Aldrich) with no Suc added to the media based on Macgregor et al. (2008). For the diurnal RNA measurements in Supplemental Figure 6 online, 0.5× MS and 1.2% agar were used. Unless noted, standard growth conditions were for 2 weeks in 12L:12D white-light cycles (80 μmol/m^2/s) at 22°C.

For delayed fluorescence and luminescence techniques a chlorine gas–based methodology was used for sterilizing seeds (Clough and Bent, 1998). The seed was then sown in groups of 10 to 20 seedlings on microtiter plates containing MS media and 1.5% agar. After 2 d at 4°C, seedlings were grown for either 6 d for luciferase experiments or 15 d for delayed fluorescence experiments in 22°C under 12L:12D white-light cycles (80 μmol/m^2/s white light). After this time in growth conditions, plates were transferred to experimental conditions at dawn of the 7th or 16th day.

DNA Constructs and Plant Transformation

The *35S:HOS1-CFP* lines were created by cloning the full-length cDNA (long isoform according to Lee et al., 2012) using ligation-independent cloning from a pET-YSBLIC3C intermediate vector (Alzari et al., 2006) into a Cambia binary vector (pPCV-CFP-H) between a 2x35S promoter and a 3′ fusion to the CFP sequence. The *HOS1* wild-type cDNA was amplified from plasmid available from the ABRC using HiTEL-HOS1 forward primer and HiTEL-HOS1 reverse primer as detailed in Supplemental Data Set 3 online. The *COR15a:LUC* transgene was made using InFusion cloning where 2.9 kb of the genomic region upstream of *COR15a* start was placed at the *Stu*I site of a pPCV-based binary vector (LUC-NOS pPCV) (Tóth et al., 2001). The primers used were pCOR15A_F and pCOR15A_R (see Supplemental Data Set 3 online). The *CAB2:LUC*+ transgene (Hall et al., 2002) and the *CCR2:LUC* transgene (Doyle et al., 2002) were previously described. *hos1-3* plants were transformed with these constructs using standard *Agrobacterium tumefaciens*–mediated transformation and selected on the appropriate antibiotics. Single insert, homozygous transgenic plants were used in all the assays.

Primers

All primers used for genotyping and qPCR are described in Supplemental Data Set 3 online. Unpublished primers were designed by hand or aided by SIGnAL iSct primers (http://signal.salk.edu/tdnaprimers.2.html) or Primer3 (Rozen and Skaletsky, 2000).

Luminescence and Delayed Fluorescence

Luciferase analysis was performed on 7-d-old seedlings, measuring luminescence every 2 h. Luciferase experimental conditions consisted of constant temperature of 12, 17, or 27°C and 2 d in 12L:12D red-light cycles followed by constant red light (30 μmol/m^2/s). Luciferase experimental conditions for Supplemental Figure 4 online were room temperature in constant white light (40 μmol/m^2/s). The delayed fluorescence technique was performed on 16-d-old seedlings, measuring delayed fluorescence every hour in 12, 17, or 27°C and constant red or blue light (30 μmol/m^2/s) (Gould et al., 2009). Both luminescence and delayed fluorescence were measured and processed as previously described (Gould et al., 2006, 2009). Data analysis was performed on Biodare (http://www.biodare.ed.ac.uk) using BRASS (available from www.amillar.org). BRASS produces individual period estimates as well as relative amplitude errors (RAEs) via fast Fourier transform nonlinear least-squares analysis (Plautz et al., 1997).

Gene Expression Analysis

For Figure 1B, plants were grown using the standard plant growth conditions described above for 10 d and harvested in triplicate at dawn into liquid nitrogen. RNA was extracted using the standard protocols for Qiagen RNeasy plant mini kit, and 1 μg of RNA was converted into cDNA using with Invitrogen's SuperScript II reverse transcriptase and oligo(dT) 12-18 primer. qPCR was performed on the resulting cDNA using Agilent Technologies Brilliant III Ultra-Fast SYBR Green qPCR master mix and ROX Passive Reference Dye on a Stratagene Mx3000P real-time PCR system with the recommended settings for SYBR Green (with dissociation curve). Data were analyzed with MxPro-Mx3005P v4.10 software. The transcript abundance levels were normalized to *UBIQUITIN10* (*UBQ10*) (Gould et al., 2006).

For the constant light time-series data in Figure 3, seeds were grown for 7 d in 12L:12D white-light cycles (80 μmol/m^2/s) at 22°C followed by 2 d in 12L:12D red-light cycles (30 to 40 μmol/m^2/s) at 17°C before being transferred to constant red light at 17°C. Seedlings were harvested in triplicate at the times indicated and frozen in liquid nitrogen. RNA was extracted and a cDNA library prepared as in Figure 2B. The qPCR was set up using a liquid handling robot (Tecan Freedom Evo) and run in a LightCycler 480 system (Roche) using LightCycler 480 SYBR green master mix (Roche). Data were analyzed with the Roche LightCycler 480SW 1.5 using advance relative quantification based on the 2nd derivative max method. Each cDNA sample was assayed in triplicate. The transcript abundance levels were normalized to *ACTIN7* (*ACT7*) (Hall et al., 2003).

For red diurnal time series data in Supplemental Figure 6 online, seedlings were grown as for Figure 3 but harvested during 12-h red light and 12-h dark cycles after a total of 13 d of growth into Ambion's RNAlater and stored at 4°C overnight. Total RNA was extracted using GE Healthcare Illustra RNAspin 96 using a liquid handling robot (Tecan Freedom Evo). RNA was extracted from three biological repeats. Total RNA (1 μg) was reverse transcribed using the Invitrogen Superscript VILO cDNA synthesis kit according to the manufacturer's instructions. qPCR analysis was done as in Figure 3.

For Figures 5 and 6, seedlings were grown for 14 d using the standard growth conditions described above and then harvested in triplicate into liquid nitrogen at the times indicated. RNA was extracted and cDNA synthesized as in Figure 2B. qPCR was performed as in Figure 2B. The transcript abundance levels were normalized to *TUBULIN BETA-9 CHAIN* (*TUB9*) (Koo et al., 2010) for the analysis in Figure 5B and *UBQ10* (Gould et al., 2006) for the analysis in Figures 5C and 6.

RNA Sequencing and Analysis

Seeds were grown for 14 d using the standard plant growth conditions described above and harvested at dawn in triplicate. RNA was extracted using the standard protocols for Qiagen RNeasy plant mini kit with the additional steps for DNase treatment. Five micrograms of RNA was submitted to sequencing using standard protocols for Illumina TruSeq (version 3) technologies. The input material was spiked with ~1% Ambion ERCC RNA spike-in mix. The resulting FASTQ files contained 262,407,174 reads for Col and 258,662,478 reads for *hos1-3*. These were then filtered using the fastq-mcf program from the ea-utils package (http://code.google.com/p/ea-utils/) with the parameters -x 0.01 -q 20 -p 10 -u. Spike-in reads were removed using Bowtie and the lower limit of detection quantified using custom scripts. The remaining reads were aligned using Tophat v1.4.1 and the following parameters: -I 10,000 -r 50–mate-std-dev 100 –library-type fr-unstranded. The TAIR10 reference sequence was used. The Cufflinks package was used to quantify gene and isoform abundance using the -G flag. The 17 cuffcompare and cuffdiff components of Cufflinks were used to quantify gene and isoform differential expression (Trapnell et al., 2012). A false discovery rate of 5% was used. All other settings were as per the default settings. Further analysis was performed using the cummeRbund package (Trapnell et al., 2012).

Hypocotyl Assays

Seeds were exposed to 2 d of 12L:12D white-light cycles to induce germination followed by 7 d at 22°C in either 12L:12D white-light cycles or constant darkness. The plates were scanned and hypocotyl lengths measured using ImageJ (http://rsbweb.nih.gov/ij/).

In Situ Hybridization

In situ hybridization was performed on plants grown in the standard growth conditions for 14 d and fixed at dawn or dusk of the 12L:12D white-light cycles. Whole-mount in situ hybridization was performed as described (Engler et al., 1994; Gong et al., 2005) with minor modifications. Microscopy was performed on the root tissues using an IX81 motorized inverted microscope (Olympus), equipped with a VS-LMS4 Laser-Merge-System with solid-state lasers (488 nm/70 mW; Visitron System). The 4′,6-diamidino-2-phenylindole (DAPI) was imaged with mercury lamp illumination of the IX81 microscope and standard DAPI filter sets (377 ± 50/406/447 ± 60). For Figure 5A, the ×40 lens and standard GFP illumination settings were used with equivalent exposure times. For Figure 5B, 5 μL of 10 μg/mL of DAPI in water was applied directly to the roots on a slide and plants were mounted in 25 μL of Vectashield. Images were taken using the ×100 lens with standard settings for the Epi488 laser and DAPI with equivalent exposure times across the images.

Protein Extraction and Immunoblotting

Protein was extracted using extraction buffer [50% ethylene glycol, 100 mM Tris-HCl, pH 8.5, 150 mM $(NH_4)_2SO_4$, 10 mM EDTA, 60 mM $NaHSO_3$, 1 mM DTT, Roche complete EDTA-free protease inhibitor cocktail, and 0.1 M phenylmethylsulfonyl fluoride]. The samples were ground in a tissue-lyzer for at least 2 min and centrifuged for 5 min at 4°C. The supernatant was removed to a new tube and kept at −80°C. Equal volumes of protein were loaded onto precast RunBlue SDS Gel 4-12% (17-wells Expedeon) and run according to the manufacturers' guidelines. Protein transfer to Invitrogen's iBlot polyvinylidene difluoride membrane was accomplished using Invitrogen's iBlot protocol using Program P3 for a total of 8 min. Once transferred, the membrane was blocked overnight and incubated with anti-LHY antibody (Kim et al., 2003) for 2 h at room temperature and probed with the secondary antibody anti-rabbit IgG–horseradish peroxidase (Insight Biotechnology SC-2004) at a 1:3000 dilution. The blot was then reprobed for UGPase using Millipore's SNAP ID Western Blotting protein detection system according to the manufacturer's protocols. The anti-UGPase rabbit polyclonal serum (Agrisera AS05-086) was used at 1:6000. Enhanced chemiluminescence quantitation was performed with Millipore's Immobilon horseradish peroxidase chemiluminescent substrate (Fisher Scientific). Detection was done using G-BOX iChemi chemical imager from Syngene set for 1-, 3-, 5-, and 10-min exposures using GeneSnap image acquisition software.

Accession Numbers

Sequence data from this article can be found in the Arabidopsis Genome Initiative or GenBank/EMBL databases under the following accession numbers: *ACT7* (At5g09810), *CAB2* (At1g29920), *CCA1* (At2g46830), *CCR2* (At2g21660), *CHE* (At5g08330), *ELF3* (At2g25930), *GI* (At1g22770), *HOS1* (At2g39810), *HST* (At3g05040), *LHY* (At1g01060), *LOS4* (At3g53110), *LUX* (At3g46640), *NUA* (At1g79280), *NUP107* (At3g14120), *PRR3* (At5g60100), *PRR5* (At5g24470), *PRR7* (At5g02810), *PRR9* (At2g46790), *RD29A* (At5g52310), *SAR1* (At1g33410), *TOC1* (At5g61380), *TUB9* (At4g20890), *UBQ10* (At4g05320), and *ZTL* (At5g57360),

Supplemental Data

The following materials are available in the online version of this article.

Supplemental Figure 1. Loss of *HOS1* in Col Leads to Early Flowering and Altered Expression of *CBF3*.

Supplemental Figure 2. The *hos1* Mutant Has a Long-Period Circadian Phenotype across a Range of Physiological Temperatures.

Supplemental Figure 3. Alleles of *hos1* in Multiple Accessions Share the Long-Period Phenotype as Measured by Delayed Fluorescence.

Supplemental Figure 4. The *hos1* Mutant Has a Long-Period Circadian Phenotype across a Range of Physiological Temperatures.

Supplemental Figure 5. The *hos1* Mutant Has a Long-Period Circadian Phenotype for *LHY*:*LUC*, *PRR9*:*LUC*, *PRR7*:*LUC*, and *TOC1*:*LUC*.

Supplemental Figure 6. *HOS1* Is Required for Wild-Type Hypocotyl Elongation and This Phenotype Does Not Require the Clock Mutants Analyzed.

Supplemental Figure 7. Constitutive Overexpression of *HOS1-CFP* in *hos1-3* Compliments the Long-Hypocotyl and Long-Period Delayed Fluorescence Phenotypes of *hos1-3*.

Supplemental Figure 8. *HOS1* Is Required for Correct Expression of Clock Genes at a Variety of Physiological Temperatures under 12L:12D Red-Light Cycles.

Supplemental Data Set 1. Genes Up- or Downregulated Two or More Fold in *hos1* Compared with Col.

Supplemental Data Set 2. AmiGO Analysis.

Supplemental Data Set 3. Primer Sequences.

ACKNOWLEDGMENTS

This work was funded by Biotechnology and Biological Science Research Council Grants BB/F005296/2 (to S.P.), BB/F005237/1 (to K.J.H.), and BB/F005318/1 (to A.J.H.). We thank Isabelle Carre for the gift of the LHY antibody.

AUTHOR CONTRIBUTIONS

D.R.M. created the stable *35S*:*HOS1-CFP Arabidopsis* lines, isolated and verified the mutant lines from the stock centers, performed RNA extractions, real-time qPCR, hypocotyl assays, and in situ hybridizations, prepared samples for and did the analysis of data resulting from RNA sequencing, and crossed in and performed the analysis of clock gene:luciferase period in *hos1* mutants, with assistance from S.B. and R.P. P.G. originally identified *hos1-3* as having a clock phenotype and performed circadian delayed fluorescence and luciferase analysis for downstream reporter:luciferase transgenic lines in *hos1* with assistance from J.Y. J.F. and J.G. performed RNA extractions and real-time PCR and created the reporter:luciferase transgenic lines in *hos1*, with assistance from G.S. and K.S. K.P. performed the bioinformatic analysis for the RNA sequencing. S.P. and A.J.H. designed experiments with contributions from A.J.M. and K.J.H. S.P., A.J.H., D.R.M., and P.G. cowrote the article with the assistance of J.F. and K.J.H. S.P., A.J.H., and K.J.H. were principal investigators on the listed grants.

Received June 14, 2013; revised October 10, 2013; accepted October 25, 2013; published November 19, 2013.

REFERENCES

Alzari, P.M., et al. (2006). Implementation of semi-automated cloning and prokaryotic expression screening: The impact of SPINE. Acta Crystallogr. D Biol. Crystallogr. **62:** 1103–1113.

Bieniawska, Z., Espinoza, C., Schlereth, A., Sulpice, R., Hincha, D.K., and Hannah, M.A. (2008). Disruption of the Arabidopsis circadian clock is responsible for extensive variation in the cold-responsive transcriptome. Plant Physiol. **147:** 263–279.

Bollman, K.M., Aukerman, M.J., Park, M.-Y., Hunter, C., Berardini, T.Z., and Poethig, R.S. (2003). HASTY, the *Arabidopsis* ortholog of exportin 5/MSN5, regulates phase change and morphogenesis. Development **130:** 1493–1504.

Braud, C., Zheng, W., and Xiao, W. (2012). LONO1 encoding a nucleoporin is required for embryogenesis and seed viability in Arabidopsis. Plant Physiol. **160:** 823–836.

Carbon, S., Ireland, A., Mungall, C.J., Shu, S., Marshall, B., and Lewis, S.AmiGO Hub; Web Presence Working Group (2009). AmiGO: Online access to ontology and annotation data. Bioinformatics **25:** 288–289.

Cernac, A., Lincoln, C., Lammer, D., and Estelle, M. (1997). The SAR1 gene of *Arabidopsis* acts downstream of the AXR1 gene in auxin response. Development **124:** 1583–1591.

Chinnusamy, V., Ohta, M., Kanrar, S., Lee, B.-H., Hong, X., Agarwal, M., and Zhu, J.-K. (2003). ICE1: A regulator of cold-induced transcriptome and freezing tolerance in *Arabidopsis*. Genes Dev. **17:** 1043–1054.

Chinnusamy, V., Zhu, J.-K., and Sunkar, R. (2010). Gene regulation during cold stress acclimation in plants, In Plant Stress Tolerance, Vol. 639 of Methods in Molecular Biology, R. Sunkar, ed (Totowa, N.J.: Humana Press) pp. 39–55.

Clarkson, W.D., Corbett, A.H., Paschal, B.M., Kent, H.M., McCoy, A.J., Gerace, L., Silver, P.A., and Stewart, M. (1997). Nuclear protein import is decreased by engineered mutants of nuclear transport factor 2 (NTF2) that do not bind GDP-Ran. J. Mol. Biol. **272:** 716–730.

Clever, M., Funakoshi, T., Mimura, Y., Takagi, M., and Imamoto, N. (2012). The nucleoporin ELYS/Mel28 regulates nuclear envelope subdomain formation in HeLa cells. Nucleus **3:** 187–199.

Clough, S.J., and Bent, A.F. (1998). Floral dip: A simplified method for Agrobacterium-mediated transformation of *Arabidopsis thaliana*. Plant J. **16:** 735–743.

Covington, M.F., Maloof, J.N., Straume, M., Kay, S.A., and Harmer, S.L. (2008). Global transcriptome analysis reveals circadian regulation of key pathways in plant growth and development. Genome Biol. **9:** R130.

Dodd, A.N., Salathia, N., Hall, A., Kévei, E., Tóth, R., Nagy, F., Hibberd, J.M., Millar, A.J., and Webb, A.A.R. (2005). Plant circadian clocks increase photosynthesis, growth, survival, and competitive advantage. Science **309:** 630–633.

Doherty, C.J., Van Buskirk, H.A., Myers, S.J., and Thomashow, M.F. (2009). Roles for *Arabidopsis* CAMTA transcription factors in cold-regulated gene expression and freezing tolerance. Plant Cell **21:** 972–984.

Dong, C.-H., Agarwal, M., Zhang, Y., Xie, Q., and Zhu, J.-K. (2006a). The negative regulator of plant cold responses, HOS1, is a RING E3 ligase that mediates the ubiquitination and degradation of ICE1. Proc. Natl. Acad. Sci. USA **103:** 8281–8286.

Dong, C.-H., Hu, X., Tang, W., Zheng, X., Kim, Y.S., Lee, B.H., and Zhu, J.-K. (2006b). A putative *Arabidopsis* nucleoporin, AtNUP160, is critical for RNA export and required for plant tolerance to cold stress. Mol. Cell. Biol. **26:** 9533–9543.

Dong, M.A., Farré, E.M., and Thomashow, M.F. (2011). Circadian clock-associated 1 and late elongated hypocotyl regulate expression of the C-repeat binding factor (CBF) pathway in *Arabidopsis*. Proc. Natl. Acad. Sci. USA **108:** 7241–7246.

Doyle, M.R., Davis, S.J., Bastow, R.M., McWatters, H.G., Kozma-Bognár, L., Nagy, F., Millar, A.J., and Amasino, R.M. (2002). The ELF4 gene controls circadian rhythms and flowering time in *Arabidopsis thaliana*. Nature **419:** 74–77.

Engler, J.A., Montagu, M., and Engler, G. (1994). Hybridization in situ of whole-mount messenger RNA in plants. Plant Mol. Biol. Rep. **12:** 321–331.

Fowler, S., and Thomashow, M.F. (2002). *Arabidopsis* transcriptome profiling indicates that multiple regulatory pathways are activated during cold acclimation in addition to the CBF cold response pathway. Plant Cell **14:** 1675–1690.

Fowler, S.G., Cook, D., and Thomashow, M.F. (2005). Low temperature induction of Arabidopsis CBF1, 2, and 3 is gated by the circadian clock. Plant Physiol. **137:** 961–968.

Gilmour, S.J., Zarka, D.G., Stockinger, E.J., Salazar, M.P., Houghton, J.M., and Thomashow, M.F. (1998). Low temperature regulation of the *Arabidopsis* CBF family of AP2 transcriptional activators as an early step in cold-induced COR gene expression. Plant J. **16:** 433–442.

Gong, Z., Dong, C.-H., Lee, H., Zhu, J., Xiong, L., Gong, D., Stevenson, B., and Zhu, J.-K. (2005). A DEAD box RNA helicase is essential for mRNA export and important for development and stress responses in *Arabidopsis*. Plant Cell **17:** 256–267.

Gong, Z., Lee, H., Xiong, L., Jagendorf, A., Stevenson, B., and Zhu, J.-K. (2002). RNA helicase-like protein as an early regulator of transcription factors for plant chilling and freezing tolerance. Proc. Natl. Acad. Sci. USA **99:** 11507–11512.

Gould, P.D., Diaz, P., Hogben, C., Kusakina, J., Salem, R., Hartwell, J., and Hall, A. (2009). Delayed fluorescence as a universal tool for the measurement of circadian rhythms in higher plants. Plant J. **58:** 893–901.

Gould, P.D., Locke, J.C., Larue, C., Southern, M.M., Davis, S.J., Hanano, S., Moyle, R., Milich, R., Putterill, J., Millar, A.J., and Hall, A. (2006). The molecular basis of temperature compensation in the *Arabidopsis* circadian clock. Plant Cell **18:** 1177–1187.

Hall, A., Bastow, R.M., Davis, S.J., Hanano, S., McWatters, H.G., Hibberd, V., Doyle, M.R., Sung, S., Halliday, K.J., Amasino, R.M., and Millar, A.J. (2003). The TIME FOR COFFEE gene maintains the amplitude and timing of *Arabidopsis* circadian clocks. Plant Cell **15:** 2719–2729.

Hall, A., Kozma-Bognár, L., Bastow, R.M., Nagy, F., and Millar, A.J. (2002). Distinct regulation of CAB and PHYB gene expression by similar circadian clocks. Plant J. **32:** 529–537.

Harmer, S.L., Hogenesch, J.B., Straume, M., Chang, H.-S., Han, B., Zhu, T., Wang, X., Kreps, J.A., and Kay, S.A. (2000). Orchestrated transcription of key pathways in *Arabidopsis* by the circadian clock. Science **290:** 2110–2113.

Hazen, S.P., Schultz, T.F., Pruneda-Paz, J.L., Borevitz, J.O., Ecker, J.R., and Kay, S.A. (2005). LUX ARRHYTHMO encodes a Myb domain protein essential for circadian rhythms. Proc. Natl. Acad. Sci. USA **102:** 10387–10392.

Hicks, K.A., Millar, A.J., Carré, I.A., Somers, D.E., Straume, M., Meeks-Wagner, D.R., and Kay, S.A. (1996). Conditional circadian dysfunction of the *Arabidopsis* early-flowering 3 mutant. Science **274:** 790–792.

Ibáñez, C., Kozarewa, I., Johansson, M., Ogren, E., Rohde, A., and Eriksson, M. (2010). Circadian clock components regulate entry and affect exit of seasonal dormancy as well as winter hardiness in Populus trees. Plant Physiol. **153:** 1823–1833.

Imaizumi, T. (2010). *Arabidopsis* circadian clock and photoperiodism: Time to think about location. Curr. Opin. Plant Biol. **13:** 83–89.

Ishitani, M., Xiong, L., Lee, H., Stevenson, B., and Zhu, J.-K. (1998). HOS1, a genetic locus involved in cold-responsive gene expression in *Arabidopsis*. Plant Cell **10:** 1151–1161.

Ishitani, M., Xiong, L., Stevenson, B., and Zhu, J.K. (1997). Genetic analysis of osmotic and cold stress signal transduction in *Arabidopsis*: Interactions and convergence of abscisic acid-dependent and abscisic acid-independent pathways. Plant Cell **9:** 1935–1949.

Ito, S., Matsushika, A., Yamada, H., Sato, S., Kato, T., Tabata, S., Yamashino, T., and Mizuno, T. (2003). Characterization of the APRR9 pseudo-response regulator belonging to the APRR1/TOC1 quintet in *Arabidopsis thaliana*. Plant Cell Physiol. **44:** 1237–1245.

Jaglo-Ottosen, K.R., Gilmour, S.J., Zarka, D.G., Schabenberger, O., and Thomashow, M.F. (1998). *Arabidopsis* CBF1 overexpression induces COR genes and enhances freezing tolerance. Science **280:** 104–106.

James, A.B., Syed, N.H., Bordage, S., Marshall, J., Nimmo, G.A., Jenkins, G.I., Herzyk, P., Brown, J.W., and Nimmo, H.G. (2012). Alternative splicing mediates responses of the *Arabidopsis* circadian clock to temperature changes. Plant Cell **24:** 961–981.

Jung, J.-H., Seo, P.J., and Park, C.-M. (2012). The E3 ubiquitin ligase HOS1 regulates *Arabidopsis* flowering by mediating CONSTANS degradation under cold stress. J. Biol. Chem. **287:** 43277–43287.

Kaczorowski, K. (2004). Mutants in Phytochrome-Dependent Seedling Photomorphogenesis and Control of the *Arabidopsis* Circadian Clock. (Berkeley, CA: University of California).

Kim, J.Y.Y., Song, H.R.R., Taylor, B.L., and Carré, I.A. (2003). Light-regulated translation mediates gated induction of the arabidopsis clock protein LHY. The EMBO J. **22:** 935–944.

Koo, S.C., et al. (2010). Control of lateral organ development and flowering time by the *Arabidopsis thaliana* MADS-box gene AGAMOUS-LIKE6. Plant J. **62:** 807–816.

Kreps, J.A., Wu, Y., Chang, H.-S., Zhu, T., Wang, X., and Harper, J.F. (2002). Transcriptome changes for Arabidopsis in response to salt, osmotic, and cold stress. Plant Physiol. **130:** 2129–2141.

Lazaro, A., Valverde, F., Piñeiro, M., and Jarillo, J.A. (2012). The *Arabidopsis* E3 ubiquitin ligase HOS1 negatively regulates CONSTANS abundance in the photoperiodic control of flowering. Plant Cell **24:** 982–999.

Lee, H., Xiong, L., Gong, Z., Ishitani, M., Stevenson, B., and Zhu, J.K. (2001). The *Arabidopsis* HOS1 gene negatively regulates cold signal transduction and encodes a RING finger protein that displays cold-regulated nucleo-cytoplasmic partitioning. Genes Dev. **15:** 912–924.

Lee, J.H., Kim, S.H., Kim, J.J., and Ahn, J.H. (2012). Alternative splicing and expression analysis of high expression of osmotically responsive genes1 (HOS1) in *Arabidopsis*. BMB Rep **45:** 515–520.

Liu, Q., Kasuga, M., Sakuma, Y., Abe, H., Miura, S., Yamaguchi-Shinozaki, K., and Shinozaki, K. (1998). Two transcription factors, DREB1 and DREB2, with an EREBP/AP2 DNA binding domain separate two cellular signal transduction pathways in drought- and low-temperature-responsive gene expression, respectively, in *Arabidopsis*. Plant Cell **10:** 1391–1406.

MacGregor, D.R., Deak, K.I., Ingram, P.A., and Malamy, J.E. (2008). Root system architecture in *Arabidopsis* grown in culture is regulated by sucrose uptake in the aerial tissues. Plant Cell **20:** 2643–2660.

Martin-Tryon, E.L., Kreps, J.A., and Harmer, S.L. (2007). GIGANTEA acts in blue light signaling and has biochemically separable roles in circadian clock and flowering time regulation. Plant Physiol. **143:** 473–486.

McClung, C.R. (2006). Plant circadian rhythms. Plant Cell **18:** 792–803.

Medina, J., Bargues, M., Terol, J., Pérez-Alonso, M., and Salinas, J. (1999). The Arabidopsis CBF gene family is composed of three genes encoding AP2 domain-containing proteins whose expression is regulated by low temperature but not by abscisic acid or dehydration. Plant Physiol. **119:** 463–470.

Michael, T.P., Salomé, P.A., Yu, H.J., Spencer, T.R., Sharp, E.L., McPeek, M.A., Alonso, J.M., Ecker, J.R., and McClung, C.R. (2003). Enhanced fitness conferred by naturally occurring variation in the circadian clock. Science **302:** 1049–1053.

Miura, K., Jin, J.B., Lee, J., Yoo, C.Y., Stirm, V., Miura, T., Ashworth, E.N., Bressan, R.A., Yun, D.-J., and Hasegawa, P.M. (2007). SIZ1-mediated sumoylation of ICE1 controls CBF3/DREB1A expression and freezing tolerance in *Arabidopsis*. Plant Cell **19:** 1403–1414.

Mockler, T.C., Michael, T.P., Priest, H.D., Shen, R., Sullivan, C.M., Givan, S.A., McEntee, C., Kay, S.A., and Chory, J. (2007). The DIURNAL project: DIURNAL and circadian expression profiling, model-based pattern matching, and promoter analysis. Cold Spring Harb. Symp. Quant. Biol. **72:** 353–363.

Nagel, D.H., and Kay, S.A. (2012). Complexity in the wiring and regulation of plant circadian networks. Curr. Biol. **22:** R648–R657.

Nakamichi, N., Kusano, M., Fukushima, A., Kita, M., Ito, S., Yamashino, T., Saito, K., Sakakibara, H., and Mizuno, T. (2009). Transcript profiling of an *Arabidopsis* PSEUDO RESPONSE REGULATOR arrhythmic triple mutant reveals a role for the circadian clock in cold stress response. Plant Cell Physiol. **50:** 447–462.

Nozue, K., Covington, M.F., Duek, P.D., Lorrain, S., Fankhauser, C., Harmer, S.L., and Maloof, J.N. (2007). Rhythmic growth explained by coincidence between internal and external cues. Nature **448:** 358–361.

Para, A., Farré, E.M., Imaizumi, T., Pruneda-Paz, J.L., Harmon, F. G., and Kay, S.A. (2007). PRR3 is a vascular regulator of TOC1 stability in the *Arabidopsis* circadian clock. Plant Cell **19:** 3462–3473.

Park, M.Y., Wu, G., Gonzalez-Sulser, A., Vaucheret, H., and Poethig, R.S. (2005). Nuclear processing and export of microRNAs in *Arabidopsis*. Proc. Natl. Acad. Sci. USA **102:** 3691–3696.

Parry, G., Ward, S., Cernac, A., Dharmasiri, S., and Estelle, M. (2006). The *Arabidopsis* SUPPRESSOR OF AUXIN RESISTANCE proteins are nucleoporins with an important role in hormone signaling and development. Plant Cell **18:** 1590–1603.

Plautz, J.D., Straume, M., Stanewsky, R., Jamison, C.F., Brandes, C., Dowse, H.B., Hall, J.C., and Kay, S.A. (1997). Quantitative analysis of Drosophila period gene transcription in living animals. J. Biol. Rhythms **12:** 204–217.

Pokhilko, A., Fernández, A.P., Edwards, K.D., Southern, M.M., Halliday, K.J., and Millar, A.J. (2012). The clock gene circuit in *Arabidopsis* includes a repressilator with additional feedback loops. Mol. Syst. Biol. **8:** 574.

Pruneda-Paz, J.L., Breton, G., Para, A., and Kay, S.A. (2009). A functional genomics approach reveals CHE as a component of the *Arabidopsis* circadian clock. Science **323:** 1481–1485.

Rozen, S., and Skaletsky, H. (2000). Primer3 on the WWW for general users and for biologist programmers. Methods Mol. Biol. **132:** 365–386.

Seo, P.J., Park, M.-J., Lim, M.-H., Kim, S.-G., Lee, M., Baldwin, I.T., and Park, C.-M. (2012). A self-regulatory circuit of CIRCADIAN CLOCK-ASSOCIATED1 underlies the circadian clock regulation of temperature responses in *Arabidopsis*. Plant Cell **24:** 2427–2442.

Sharabi-Schwager, M., Lers, A., Samach, A., Guy, C.L., and Porat, R. (2010). Overexpression of the CBF2 transcriptional activator in *Arabidopsis* delays leaf senescence and extends plant longevity. J. Exp. Bot. **61:** 261–273.

Stockinger, E.J., Gilmour, S.J., and Thomashow, M.F. (1997). *Arabidopsis thaliana* CBF1 encodes an AP2 domain-containing transcriptional activator that binds to the C-repeat/DRE, a cis-acting DNA regulatory element that stimulates transcription in response to low temperature and water deficit. Proc. Natl. Acad. Sci. USA **94:** 1035–1040.

Straszer, K., and Hurt, E. (2000). Yra1p, a conserved nuclear RNA-binding protein, interacts directly with mex67p and is required for mRNA export. The EMBO Journal **19:** 410–420.

Tamura, K., Fukao, Y., Iwamoto, M., Haraguchi, T., and Hara-Nishimura, I. (2010). Identification and characterization of nuclear pore complex components in *Arabidopsis thaliana*. Plant Cell **22:** 4084–4097.

Tóth, R., Kevei, E., Hall, A., Millar, A.J., Nagy, F., and Kozma-Bognár, L. (2001). Circadian clock-regulated expression of phytochrome and cryptochrome genes in Arabidopsis. Plant Physiol. **127:** 1607–1616.

Tourrière, H., Chebli, K., and Tazi, J. (2002). mRNA degradation machines in eukaryotic cells. Biochimie **84:** 821–837.

Trapnell, C., Roberts, A., Goff, L., Pertea, G., Kim, D., Kelley, D.R., Pimentel, H., Salzberg, S.L., Rinn, J.L., and Pachter, L. (2012). Differential gene and transcript expression analysis of RNA-seq experiments with TopHat and Cufflinks. Nat. Protoc. **7:** 562–578.

Wiermer, M., Cheng, Y.T., Imkampe, J., Li, M., Wang, D., Lipka, V., and Li, X. (2012). Putative members of the *Arabidopsis* Nup107-160 nuclear pore sub-complex contribute to pathogen defense. Plant J. **70:** 796–808.

Xu, X.M., Rose, A., Muthuswamy, S., Jeong, S.Y., Venkatakrishnan, S., Zhao, Q., and Meier, I. (2007a). NUCLEAR PORE ANCHOR, the *Arabidopsis* homolog of Tpr/Mlp1/Mlp2/megator, is involved in mRNA export and SUMO homeostasis and affects diverse aspects of plant development. Plant Cell **19:** 1537–1548.

Yamamoto, Y., Sato, E., Shimizu, T., Nakamich, N., Sato, S., Kato, T., Tabata, S., Nagatani, A., Yamashino, T., and Mizuno, T. (2003). Comparative genetic studies on the APRR5 and APRR7 genes belonging to the APRR1/TOC1 quintet implicated in circadian rhythm, control of flowering time, and early photomorphogenesis. Plant Cell Physiol. **44:** 1119–1130.

Yang, T., Chaudhuri, S., Yang, L., Du, L., and Poovaiah, B.W. (2010). A calcium/calmodulin-regulated member of the receptor-like kinase family confers cold tolerance in plants. J. Biol. Chem. **285:** 7119–7126.

Zhu, J., Shi, H., Lee, B.H., Damsz, B., Cheng, S., Stirm, V., Zhu, J.-K., Hasegawa, P.M., and Bressan, R.A. (2004). An *Arabidopsis* homeodomain transcription factor gene, HOS9, mediates cold tolerance through a CBF-independent pathway. Proc. Natl. Acad. Sci. USA **101:** 9873–9878.